Science and Technology Indonesia
e-ISSN:2580-4391 *p*-ISSN:2580-4405
Vol. 7, No. 3, July 2022

Review Paper

Crystal Engineering Approach in Physicochemical Properties Modifications of Phytochemicals

Dhea Sultana Lutfiyah[1], Lili Fitriani[1], Muhammad Taher[2], Erizal Zaini[1]*

[1]*Departement of Pharmaceutics, Faculty of Pharmacy, Andalas University, Padang, 25163, Indonesia*
[2]*Kulliyyah of Pharmacy, International Islamic University Malaysia, Kuantan, 25200, Malaysia*
***Corresponding author**: erizal@phar.unand.ac.id*

Abstract
Phytochemicals have been used to reduce the risk of diseases and maintain good health and well-being. However, most phytochemicals have a limitation in their physicochemical properties, which can be modified by reforming the shape of the crystals. Therefore, crystal engineering is a promising approach to optimize physicochemical characteristics of the active pharmaceutical ingredients (APIs) in a phytochemical without altering its pharmacological efficacy. Hence, this paper reviews current strategies for the use of crystal engineering to optimize physicochemical properties of phytochemicals, which is followed by the design of the synthesis and characterization of particular phytochemicals, including *piperine* (PIP), *quercetin* (QUE), *curcumin* (CUR), *genistein* (GEN), and *myricetin* (MYR). The literature indicates that crystal engineering of multicomponent crystals (MCCs) enhances phytochemical physicochemical properties, including solubility, dissolution rate, stability, and permeability. The MCCs provide a lower lattice energy and noncovalent bonding, which translate into lower melting points and weak intermolecular interactions that generate greater solubility, higher dissolution rate, and better stability of the APIs. Nevertheless, the absence of reported studies of phytochemical crystal engineering leads to a lack of variation in the selection of coformers, methods of preparation, and improvement of physicochemical properties. Therefore, more extensive evaluation of the design and physicochemical characteristics of phytochemicals using MCCs is necessary and manifests the opportunity to enhance the application of phytochemicals in the pharmaceutical industry.

Keywords
Phytochemical, Multicomponent Crystal, Cocrystal, Physicochemical Properties, Solubility, Dissolution Rate

Received: 17 March 2022, Accepted: 2 July 2022
https://doi.org/10.26554/sti.2022.7.3.353-371

1. INTRODUCTION

Phytochemicals, also known as secondary metabolites, are plant-derived chemicals that may benefit human health (Egbuna et al., 2019). Phytochemicals that are found in food products and benefit human health are known as nutraceuticals. According to the Association of American Feed Control Officials, nutraceuticals have been proven scientifically to be beneficial for pet health (Nwosu and Ubaoji, 2020). Currently, nutraceuticals have been used widely in the form of dietary supplements, herbal products, functional foods, nutritional isolates (B. Arnao and Hernández-Ruiz, 2018), probiotics, and prebiotics (Nwosu and Ubaoji, 2020). These products each have been recognized for their ability to reduce the risk of disease and contribute to the treatment of various medical conditions. For example, there are reports of the use of *curcumin* (CUR) from turmeric as an adjunctive treatment for cancer patients (Jiao et al., 2016; Seo et al., 2016), *quercetin* (QUE) in maintaining glucose for patients with diabetes (Lee et al., 2012; Nguyen et al., 2015), and many other clinical activities.

Despite the positive contributions to the state of human health, research data indicates that the global market in Association of Southeast Asian Nations countries has become a niche market in the most rapid expansion of the phytochemical industry (Kantatasiri, 2012). Immunity boosters, cholesterol-lowering agents, joint and heart care, collagen, fat-burning supplements are some of best-selling phytochemicals worldwide (Toyoda et al., 2016). However, the majority of phytochemicals have challenges that affect their bioactivity: limited aqueous solubility and dissolution rate, high melting point, hygroscopicity, and chemical instability (McClements, 2012; Yan et al., 2013).

One strategy to maximize the bioactivities of phytochemicals and to protect them against chemical, physical, or biological degradation is to deliver them to a specific site of action. Various approaches have been developed to address these challenges, presenting advantages and disadvantages with respect

to phytochemical physicochemical properties, which depend on physical, chemical, and mechanical characteristics of the active pharmaceutical ingredients (APIs) and the simplicity and efficacy of the industrial process. Moreover, studies have confirmed that optimizing the physicochemical properties of bioactive compounds may enhance the bioavailabilities and pharmacological activities of these compounds (Stasiłowicz et al., 2021).

Crystal engineering is a promising and unique approach (Liu et al., 2016a) among techniques to enhance phytochemical solubility and dissolution rates. Crystal engineering of multicomponent crystal (MCC) forms optimizes the physicochemical characteristics of a compound, such as melting point, solubility, dissolution rate, stability, permeability, and compressibility, without altering its pharmacological efficacy (Kumar, 2018). Moreover, MCC technology has been extensively researched, as demonstrated by the various coformers, methods, and types of MCCs that have been successfully formulated. Therefore, to optimize the development of phytochemicals for use in clinical and industrial pharmacy applications, this study reviews current studies on the modification of physicochemical properties using crystal engineering. The methods to synthesize and characterize MCCs will be explained to demonstrate how crystal engineering can enhance the solubility, dissolution rate, and bioavailability of selected phytochemical MCCs, including *piperine* (PIP), QUE, CUR, *genistein* (GEN), and *myricetin* (MYR). This review was performed by combining related keywords with Boolean operators to search Google Scholar and PubMed Central databases and select the literature from the past 10 years from that compiled the specific criteria, including being published in the years 2012–2022, indexed in Scopus, published in English, and complete in structure.

2. PHARMACEUTICAL CRYSTAL ENGINEERING

Crystal engineering, also known as solid-state supramolecular synthesis, is defined as "the understanding of intermolecular interactions in the context of crystal packing and the utilization of such understanding in design of new solids with desired physical and chemical properties" (Batisai, 2021; Clarke, 2012). Briefly, crystal engineering is a design strategy in the formation of MCCs that involves molecular arrangements and intermolecular interactions.

An MCC is formed by two or more different ions or molecules that solidify together as a single-phase crystalline material (Lombard et al., 2020). An MCC that is composed of a solvent or liquid as a single crystallizing unit is called as solvate. If the solvent is a water molecule, the MCC is called a hydrate. Additionally, a salt composed of two or more oppositely charged ions that crystallized and formed a neutral compound, as shown in Figure 1. Salt formation is commonly utilized for poorly water-soluble drugs containing ionizable groups, which are estimated to comprise more than 50% of drugs on the market (Batisai, 2021). Salt crystals tend to provide a larger improvement in solubility when compared with cocrystals (see below) (Zaini et al., 2019); however, their formation is not achievable for nonionizable entities that cannot form salts with counter ions.

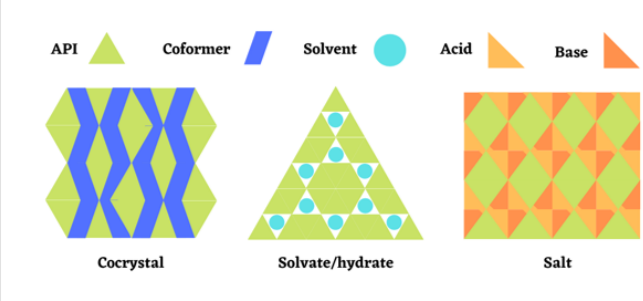

Figure 1. Types of Multicomponent Crystals

In contrast to salts, neutral molecules that are composed of APIs and selected coformers that crystallize in a definite stoichiometric ratio are known as cocrystals (Figure 1). The main guidance for selecting coformers in pharmaceutical MCC design is to use approved those that are generally recognized as safe by the United States Food and Drug Administration (FDA) and will not affect the pharmacological activities of the APIs (Thayyil et al., 2020). Several studies have revealed correlations between coformer solubility and cocrystal solubility. Thus, coformers may be selected based on solubility and the cocrystals likely possess complementary functional groups. This is the basis of applied approaches to selecting coformers using hydrogen (H) bonding propensity; performing thermal analysis; measuring saturation temperature; calculating lattice energy; using the Hansen solubility parameter; and performing synthon matching. Moreover, the type of MCCs formed can be approximated by calculating the difference in pKa values of an API and a coformer; this process is referred to pKa-based modeling. Furthermore, computational methods, such as determining supramolecular compatibility using the Cambridge Structure Database; screening of virtual cocrystals based on molecular electrostatic potential surfaces; and using the conductor-like screening model for real solvents, has also been used to select appropriate coformers for MCCs (Kumar, 2018; Sathisaran and Dalvi, 2017). In addition, lattice energies or free energy requirements for solubilization also influence the dissolution of the solid phase (Sathisaran and Dalvi, 2017). Nevertheless, physicochemical properties of cocrystal formation may depend on the method, solvent, ratio, and other factors that are not explained by the sharing of complementary functional groups between the API and the coformer. This unpredictable outcome is one of the greatest challenges when using the crystal engineering approach. Therefore, many experiments have focused on the preparation of MCCs from specific APIs.

Generally, preparation of MCCs can be classified into two methods, as shown in Figure 2, that are described in detail in this section. Once the MCC is formed, it is characterized with Fourier transformation infrared (FT-IR) spectroscopy, Fourier transformation Raman (FT-Raman) spectroscopy, single-crys-

tal X-ray diffraction (SCXRD), powder X-ray diffraction (PXRD), solid-state nuclear magnetic resonance spectroscopy, scanning electron microscopy (SEM), hot stage microscopy (HSM), thermogravimetric analysis (including differential scanning calorimetry [DSC] and differential thermal analysis [DTA]), analysis of complexation stoichiometry (CS) and electrostatic charge (EC), computations, and other related process to confirm the formation of MCCs.

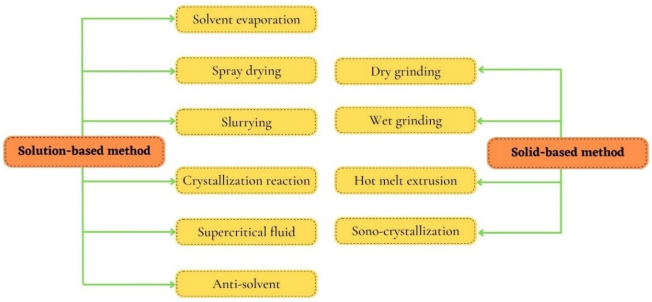

Figure 2. Category of Multicomponent Crystal Preparation Methods

2.1 Solution-Based MCC Preparation Methods

The most commonly used technique for preparing phytochemical MCCs using the solution-based method is solvent evaporation (Katherine et al., 2018; Setyawan et al., 2018; Zaini et al., 2020b), in which the API and coformer are dissolved with a suitable solvent and the solvent is then allowed to evaporate slowly at room temperature (Kumar, 2018). The second technique is spray drying, which is carried out by spraying a dissolved mixture of an API and a coformer into a hot stream; the solvent thus evaporates and MCCs form. This method was successful in producing MCCs of theophylline with citric acid, flufenamic acid, and saccharin (Hadi, 2015). Another technique used in the successful production of cocrystals of PIP with succinic acid is slurrying (Zaini et al., 2020b): the API and a suitable coformer are stirred together while a solvent is added to form a slurry, and the solvent is then decanted at room temperature to obtain dry crystals (Kumar, 2018). In the crystallization reaction method, an API that has been purified with organic solvents is added to small quantities (that do not exceed the solubility limit) of a coformer; pure cocrystals will be the precipitate in the solution (Kumar, 2018). In the supercritical fluid processing method, MCCs are formed by dissolving APIs and coformers with a high-pressure supercritical fluid (for example, the commonly used CO_2) in a stainless steel vessel (Thayyil et al., 2020). This was applied in producing CUR cocrystals using resveratrol as a coformer (Dal Magro et al., 2021). In addition, the antisolvent cocrystallization method uses an organic solvent or buffer as an antisolvent to dissolve coformers that will disperse with the APIs and other substances dissolved in the antisolvent. This achieves supersaturation and the formation of MCCs, such as that seen with CUR and dextrose cocrystals (Katherine et al., 2018; Raza et al., 2018; Sathisaran and Dalvi, 2017).

2.2 Solid-Based MCC Preparation Methods

The first method in solid-based is dry grinding, also known as mechanochemical grinding, which is conducted by crushing APIs and coformers together using a mortar and pestle or a grinder with addition of heat energy (Thayyil et al., 2020). This method was used in the successful production of MCCs of PIP with β-cyclodextrin (Quilaqueo et al., 2019). Wet grinding (also known as liquid-assisted grinding) is a similar technique, but it requires an addition of small quantities of solvent that act as a catalyst in the formation of MCCs (Gadade and Pekamwar, 2016). This is commonly used in producing MCCs of phytochemicals, such as cocrystals of QUE with succinic acid (Athiyah et al., 2019). Another method is the hot melt extrusion method, in which MCCs are formed by inducing heat during the mixing of the APIs and coformers, replacing solvents in the role of decreasing surface tension, until the API and coformer form a liquid state (Boksa et al., 2014; Gajda et al., 2019; Savjani, 2015). The last method is sonocrystallization, which was used in the successful production of cocrystals of MYR with proline (Liu et al., 2016a). Sonocrystallization is conducted by dissolving an API and coformer in a specific solvent, sonicating the solution with a sonoreactor, and leaving the solution overnight to form dry crystals (Karagianni et al., 2018; Kumar, 2018). Therefore, compared to solution-based methods, solid-based methods use relatively small amounts of or no solvent, which could minimize the probability of forming a solvate and increase the solubility by decreasing the crystallinity of the MCCs.

3. IMPACT OF MULTICOMPONENT CRYSTAL IN PHYSICOCHEMICAL PROPERTIES

MCCs primarily affect solubility and dissolution rate in the modification of physicochemical properties of APIs. Nevertheless, MCCs are also reported to improve the stability, permeability, compressibility, and palatability of certain APIs, properties that are correlated with increases in drug biovailability and therapeutic activity.

3.1 Solubility and Dissolution Rate

The solubility and dissolution rate are the most important physicochemical properties because the bioavailability of Biopharmaceutics Classification System (BCS) class II and IV APIs depends on these parameters. In general, solubility is defined as concentration of solute in a saturated solution at a certain temperature and pressure. This phenomenon involves lattice energy and solute-solvent interactions. MCCs have the effect of lowering lattice energy and solution energy, thereby decreasing the free energy of solution and improving the solubility. When the drug absorption process is limited by dissolution, enhancing solubility can increase dissolution rate and thus improve

bioavailability (Roy et al., 2012). The dissolution rate denotes the ability of a drug to dissolve at a certain time and achieve a therapeutic dose. This relates to solubility by the Nernst-Brunner or Noyes-Whitney equation as shown in Equation 1, which is:

$$\frac{dM}{dt} = \frac{D.A}{h}(Cs - Ct) \quad (1)$$

where dM/dt is dissolution rate, D is diffusion coefficient, A is solid surface area, h is thickness of diffusion layer, Cs and Ct are concentration of drug in solution at equilibrium and time t (Hadi, 2015).

Various approaches have been employed to improve the solubility of APIs, but no methods simultaneously improve the aqueous solubility and permeability of APIs without changing the APIs molecular structure (Yan et al., 2013) and affect its pharmacological active sites. Creation of MCCs is a relatively novel approach reported to enhance a material's solubility, as well as its dissolution rate (Nascimento et al., 2021; Yang et al., 2020), through improving its physicochemical properties without altering its pharmacological activity.

3.2 Stability

To enhance the bioavailability of APIs, one problem that the use of MCCs could address is improving the stability of certain APIs. Stability studies are utilized to obtain information regarding the shelf life of medicinal products through testing the products under various storage conditions. Environmental factors included as the variables in stability studies are temperature, humidity, and light at certain time intervals. Various studies have indicated promising results in stability studies of phytochemical MCCs. Yang et al. (2020) reported the stability of berberine cocrystals with fumaric acid detected with pressure measurement and the dynamic vapor sorption method and found that increasing solubility is associated with the stability of berberine in high temperature and humidity conditions.

3.3 Permeability

Another key physicochemical property to consider in drug development is permeability. The permeability of an API is an important factor that can seriously influence its bioavailability, particulary for BCS class III & IV compounds. However, several studies have reported potential enhancement of drug permeability through the formation of MCCs. For instance, a study using acyclovir as an API with poor permeability and an inability to penetrate the skin demonstrated that in vitro skin permeation was enhanced via the formation of cocrystals using fumaric acid and glutaric acid as coformers (Yan et al., 2013). Enhancement of permeability is related to higher log P values and lower melting points, which could be achieved by the formation of MCCs.

3.4 Compressibility & Palatability

Good compressibility of a dosage form is needed to encourage drug development in industrial pharmacy. Optimization of particle size and density generally leads to a corresponding improvement in compressibility (Yusof et al., 2015). In a study by Sun et al. (2019) the formulation of caffeine (CAF) and methyl gallate in a cocrystal form provides increased compressibility to CAF tablets. This finding was supported by a tensile strength study showing that the CAF-methyl gallate cocrystal tablet has a tensile strength two times higher than the single CAF compound (Al-Dulaimi et al., 2022). Moreover, palatability or taste-masking of oral preparations are additional properties modified through the addition of specific coformers. Artificial sweeterners like saccharin have been widely used as coformers in cocyrstallization. The coformer acts as a mask for the bitter taste of the API, in addition to the effect of cocrystallization itself. Maeno et al. (2014) reported research on the formation of a cocrystal of paracetamol with trimethylglycine that successfully masked the taste of paracetamol in addition to increasing compressibility and tabletability and improving the dissolution profile. Therefore, cocrystal are used to enhance the bioavailability and clinical used of phytochemicals as pharmaceuticals and nutraceuticals.

4. MULTICOMPONENT CRYSAL OF PHYTOCHEMICALS

In our previous studies, cocrystal of the phytochemical PIP modified with various coformers and preparation methods exhibited improved physicochemical properties (Jessica et al., 2021; Salsabila et al., 2021; Zaini et al., 2020a; Zaini et al., 2020b). In other reported studies, MCCs of QUE, GEN, and MYR also exhibited significant improvement in physicochemical properties over other flavonoids (Sowa et al., 2013b; Wu et al., 2020; Zhang et al., 2017b). Moreover, CUR is widely used in experimental studies of MCC, although tertiary literature that reviews it comprehensively is lacking. Therefore, among all the nonpolar, semipolar, and polar phytochemical compounds used to formulate MCCs, PIP, CUR, GEN, QUE, and MYR were the APIs selected for further review, which are shown in Figure 3.

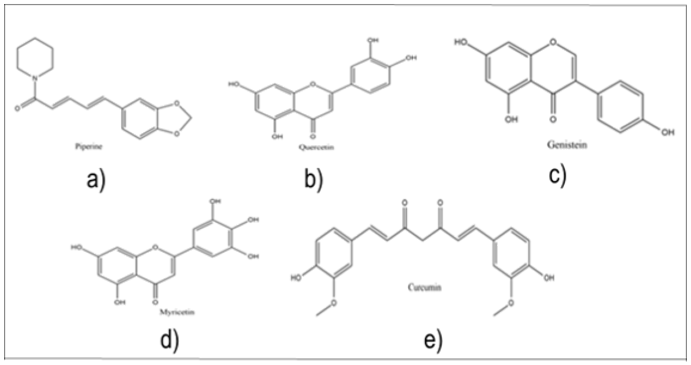

Figure 3. Chemical Structure of (a) *Piperine* (PIP), (b) *Quercetin* (QUE), (c) *Genistein* (GEN), (d) *Myricetin* (MYR), and (e) *Curcumin* (CUR)

4.1 Nonpolar Compounds

4.1.1 *Piperine* (PIP)

PIP is an alkaloid present as the main compound in black pepper (*Piper nigrum*) and long pepper (*Piper longum*) in family of Piperaceae (Gorgani et al., 2017; Ren et al., 2019; Stasiłowicz et al., 2021). PIP is not only used as a cooking spice; it also has potential therapeutic effects, such as anti-inflammatory (Bhalekar et al., 2017; Toyoda et al., 2016; Zhai et al., 2016), antioxidant, antibacterial (Zarai et al., 2013), anticancer (Gajda et al., 2019; Ouyang et al., 2013; Yaffe et al., 2015), anticonvulsant (Da Cruz et al., 2013), antidepressant (Mao et al., 2014), antidiabetic (Kharbanda et al., 2016), and antiepileptic (Chen et al., 2013a) effects, in various disease states. These therapeutic potentials of PIP have not been fully utilized because of its low solubility in water (40 μg/mL, 18°C) and toxicity at high concentrations (Pachauri et al., 2015). The low bioavailability of PIP is also affected by the rate of dissolution, which becomes rate-limiting step for the solubility for compounds poorly soluble in water (Zaini et al., 2020a). Several approaches to enhance the solubility and dissolution rate of PIP, such as nanoparticles (Bhalekar et al., 2017), solid dispersions (Thenmozhi and Yoo, 2017), inclusion complexes (Stasiłowicz et al., 2021), and MCCs (Zaini et al., 2020b), have been tested. In the application of crystal engineering, MCCs are considered to provide the most optimal results in enhancing the physicochemical properties of PIP, as seen in Table 1.

As reported by Zaini et al. (2020a) MCCs of PIP with succinic acid (SA) in 2:1 molar ratio were successfully created using the slurry method (Zaini et al., 2020a). SA was selected as the coformer because of its two carboxylic acid (-COOH) groups that are likely donate protons to one carbonyl (-C=O) group in PIP to form cocrystals (Figure 4). The cocrystal of PIP-SA was nearly four times more soluble than intact PIP (11.71 µg/mL vs. 2.93 µg/mL) in CO_2-free distilled water. This was caused by a lower melting point and channel motif formation in the crystal structure of PIP-SA. The stability of the PIP-SA cocrystal was also confirmed, as indicated by the absence of changes between the time before and after the PXRD diffractogram. Moreover, the dissolution rate of PIP-SA was higher: where 99.00% of PIP-SA dissolved, compared with intact PIP and the physical mixture (PM), of which only 42.30% and 62.22%, respectively, dissolved (Zaini et al., 2020b).

In another study by Zaini et al. (2020b) saccharine (SAC) was also reported as successful in the formation of salt with PIP in a 1:1 molar ratio using the solvent evaporation method. SAC was selected as the coformer in this case because of the presence of amine (N-H) and sulfide (S=O) functional groups that would act as H-bond donors to C=O and C-H groups in PIP to form N-H.O=C and C-H.O=S bonds. In this study, the PIP-SAC salt was nearly two times more soluble than intact PIP in acetonitrile:water (90:10). This enhancement was explained by the higher solvation of the salt type in water that would easily dissociate into anion and cation (Zaini et al., 2020b).

In addition, the use of cyclodextrin (CD) as a coformer has been extensively studied. The study by Stasiłowicz et al. (2021) reported the possibility of intermolecular PIP and hydroxypropyl-β-CD (HP-β-CD) interactions through PIP adhesion on the surface of CD . In a study by Ezawa et al. (2016) it was also suggested that intermolecular interaction occur between PIP and β-CD inclusion complexes in 1:1 and 1:2 molar ratios (Figure 4). Therefore, dissolution profile of inclusion complexes of PIP-β-CD (1:1) was dramatically enhanced in distilled water. There was no change in concentration in intact PIP and ground PIP (grinded intact PIP), albeit there was increasing surface area of ground PIP (Ezawa et al., 2016). Compared with PM, a higher percentage of PIP-HP-β-CD (6.82 vs. 7.82%) inclusion complexes was shown to be dissolved, whereas it was doubled compared with intact PIP (4.35%). Furthermore, PIP-HP-β-CD also proved to enhance PIP permeability in the parallel artificial membrane permeability assay model: the P_{app} value increased 1.36-fold (meaning, highly permeable) in gastrointestinal transite and 2-fold (meaning, moderately permeable) in the blood-brain barrier (Stasiłowicz et al., 2021).

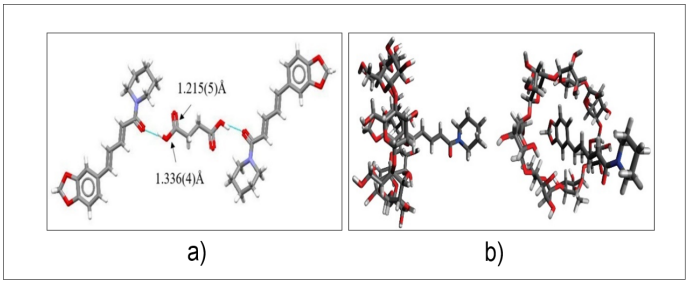

Figure 4. Intermolecular Reaction of PIP-SA (a) and PIP-β-CD (b). Reprinted with Permission of Ref (Ezawa et al., 2016; Zaini et al., 2020a) As Open Access Articles

4.1.2 *Curcumin* (CUR)

CUR is a polyphenolic compound extracted from turmeric (*Curcuma longa*) rhizomes and is widely used as a natural food coloring (Jäger et al., 2014). CUR has potential as anticancer (Jiao et al., 2016; Seo et al., 2016), antioxidant (Malik et al., 2014), anti-inflammatory (Ribas et al., 2019), antimicrobial (Balan et al., 2016), hepatoprotector (Salama et al., 2013), anti-Alzheimer's (Rao et al., 2012), and gastrointestinal protective agents (Thong-Ngam et al., 2012). However, limited clinical use of CUR relates to difficulties in its formulation because of its low solubility and bioavailability in aqueous media (0.6 μg/mL) (Katherine et al., 2018). Several approaches have also been pursued to increase CUR bioactivity, such as lipophilic matrices (Jäger et al., 2014), liposomes (Hasan et al., 2014), nanoparticles (Pandit et al., 2015; Quiñones et al., 2018), nanocapsules (Alippilakkotte and Sreejith, 2018; Pan et al., 2013), bionanoemulsions (Malik et al., 2014), and MCCs (Dal Magro et al., 2021; Katherine et al., 2018; Pang et al., 2019; Pantwalawalkar et al., 2021; Rathi et al., 2019; Ribas et al., 2019; Sathisaran and Dalvi, 2017). MCCs of CUR have been studied widely in the crystal engineering approach, as shown in Table 1.

MCCs of CUR have been produced conventionally with

Table 1. The inference of phytochemicals PIP, QUE, CUR, GEN, and MYR multicomponent crystals with various coformers including SA, SAC, HP-β-CD, β-CD, NM, MA, BYP, AA, DX, RSV, CA, CAF, INM, PRL, and PRC

API	Co-former	Ratio	Type	Method	Characterizations	Advances	Ref
PIP	SA	2:1	Co-crystal	Slurry	• PXRD: distinct and unique pattern of 2θ at eight values • DSC: lower melting point than raw PIP at 110.49°C • FR-IR S: new peaks at 2,963 and 2,600 cm^{-1} • SCXRD: neutral form of cocrystal that represented by the distance between C=O and C-OH of SA	Greater solubility, faster dissolution rate than intact PIP in CO_2-free distilled water, and passed stability test (under 40°C with %RH 75 & 100)	(Zaini et al., 2020b)
PIP	SAC	1:1	Salt	Solvent evaporation	• SEM: polyhedral shape, while PIP and SAC shows rod and depicts irregular crystal • PXRD: unique new peaks 2θ at four values • DSC: two endotherm peaks at 110.56°C (as dehydration process) and 197.09°C (as crystalline phase) melting point • FT-IR: stronger and broader changes band that estimated because of interaction between N-H.O=C and C-H.O=S	Enhancement in dissolution rate almost two times more than intact PIP	(Zaini et al., 2020a)
PIP	HP-β-CD	1:1	Inclusion complex	Kneading	• PXRD: superimposed diffraction patterns • DSC: lower melting point at 128.5°C while enthalpy higher than raw PIP • FT-IR: similarity presence peak at 3,400 cm^{-1} (for PIP-HP-β-CD) suggested as H-bond • ^{13}C-NMR: virtually indistinguishable and mixing spectra of PIP and HP-β-CD	Improvement of solubility and dissolution rate (doubled than intact PIP), higher permeability through GIT & BBB membrane	(Stasilowicz et al., 2021)
PIP	β-CD	1:1 1:2 2:1	Inclusion complex	Cogrinding process	• DSC: ground mixture (GM) of PIP-β-CD 1:1 and 1:2 disappearing PIP melting point in their curves • PXRD: halo patterns in GM 1:1 & 1:2 which confirmed amorphous state • CS: max. absorbance of PIP/ PIP + HP-β-CD in 0.5-mole fraction by Job's plot • FT-Raman: broaden and shifted to lower frequencies scattering peaks • SEM: rougher surface and agglomeration of GMs differed from raw PIP & β-CD • ^{1}H-^{1}H NOESY NMR: presented PIP protons at benzene & ester groups interacted with protons of β-CD cavity	Solubility and dissolution rate of PIP in water enhanced dramatically, while there were no changes involved to increased of surface area	(Ezawa et al., 2016)

API	Co-former	Ratio	Type	Method	Characterizations	Advances	Ref
CUR	AA	0.5-, 0.55-, 0.6-, and 0.65-mole	Co-crystal	Solvent evaporation	• DSC: endotherm peak of 0.5-, 0.6-, and 0.65-mole at 186.49, 183.03–187.10, and 185.73–188.82°C • PXRD: disappearing characteristic peaks of CUR & AA, exhibiting new reflections, and addition of characeristic feature in background • FT-IR: slightly shifted peak to lower wavenumber	Enhanced solubility of CUR in distilled water (576-fold), buffer pH 1.2 (10-fold), and buffer pH 6.8 (9-fold) that lead to superior CUR dissolution compared with pure CUR	(Pantwalawalkar et al., 2021)
CUR	DX	-	Co-crystal	Anti-solvent	• SEM: 2 shapes which long flakes (length 10–20 μm, width 2.5 μm), and round with some aggregates (CUR distributed unevenly) • FT-IR: comparable size & width as DX peak, slightly shifted to the lower wavenumber • DSC: melting point at 159.4°C which slightly shifted to lower temperature compared with CUR & DX	Cocrystallization more efficient at low concentration of CUR, increased solubility (up to 23,000 μg/mL) in water, and more stable in pH range 1–7 than pure CUR	(Katherine et al., 2018)
CUR	RSV	1:1	Co-crystal	Super-critical solvent (CSS)	• DSC: single endotherm peak at 170.4°C, which lower than CUR & RSV at 174.3°C & 277.3°C • PXRD: some characteristic peaks of CUR & RSV disappeared, reduced intensity, and widening diffraction peaks • FT-IR, cocrystal spectra showed strecthing of bands corresponding to O-H and C=C aromatic	Higher solubility than pure CUR & RSV in water, PBS, and 0.1M HCl. Reached 1.27% and 41.89% of CUR and RSV CD, which 2.28 and 2 times higher than pure CUR & RSV	(Dal Magro et al., 2021)
CUR	CA	0.3-mole	Co-crystal	Solvent evaporation	• DSC: endotherm peak of cocrystal melting point at 123°C • PXRD: new and major characteristic peaks at five 2θ values • EC: formation of H-bond between C=O (EC = -0.389) of CA with phenolic of CUR • FT-IR: involvement of -COOH group in H-bond formation because of conjugation of C=O group • SEM: distorted oval morphology (50 μm) and slightly porous nature	Cocrystal formed at 0.3-mole fraction, while 0.15- and 0.33-mole formed eutectics	(Rathi et al., 2019)
GEN	CAF	1:1	Co-crystal	Solvent-drop grinding, solvent evaporation, slurry	• FR-Raman: shifted vibrational bands as compared with starting materials • PXRD: a set of new reflections as compared with starting materials • SCXRD: asymetric unit of cocrystal comprises 1 GEN and 1 CAF molecule in neutral forms exhibited 1 H-bond (H_7-O_{2A}), 2 weaker (H_{3A1}-O_7 and H_8-O_{2A}) contacts between GEN & CAF, and intramolecular H-bond (H_5-O_4) of GEN • TG-DTA: stability of cocrysalline phase up to 247°C	More soluble than intact GEN determined by the higher Smax reached 0.861 compared with 588 μg/mL, also thermodynamically stable	(Sowa et al., 2014b)

API	Co-former	Ratio	Type	Method	Characterizations	Advances	Ref
GEN	BYP	1:1	Co-crystal	Solvent evaporation	• SCXRD: asymmetric unit comprises 1 GEN molecule & 1 BYP molecule in their neutral forms formed by strong intramolecular H-bond in GEN molecule, two intermolecular H-bonds (H-N) between GEN & BYP, and interchain H-bonds (H-O) between GEN molecules • TG-DTA: stability of cocrystalline phase up to 270°C • DSC: sharp & narrow endotherm peak at 273.9°C, which is lower than GEN (309°C), albeit higher than BYP (114°C) • PXRD: closesly match with its simulation measured patterns • IR: changed of positions, intensities, and shapes of bands at 400-4000 cm^{-1}	More soluble than intact GEN determined by the higher Smax reached at 23.44 compared with 15.71 μg/mL after 130 min compared with 240 min. Moreover, showed antibacterial activity against *Staphylococcus aureus* and *Escherichia coli*	(Zhang et al., 2017b)
GEN	NM	1:1	Co-crystal	Solvent evaporation	• PXRD: conversion into a cocrystalline phase pattern • SCXRD: asymmetric unit contains of one GEN, one NM, and one water molecule formed a three-component molecular assembly via H-bonding • FT-Raman: stretching vibrations of C=O groups, and simultaneous change in positions and shapes of -OH groups bands • TG-DTA & DSC: broadened exotherm of DSC (at 89.3°C), dehydration gradually over 80–115°C, and decomposition subsequent to dehydration	Successed application of pyridinecarboxamide coformers in cocrystallization	(Sowa et al., 2013b)
GEN	1NM	1:2	Co-crystal	Solvent evaporation	• CSA: GEN contains three potential sites with H-bonding donor • Computations: Hirshfeld surface presented 2D OH-O, NH-O, and OH-N hydrogen-bonded layers that combined by multidirectional π-π interactions to form 3D lattice	Illustrates the differences of two molecules of INM environments by analysis of Hirshfeld surfaces and various types of contact contributed	(Sowa et al., 2013a)
QUE	SA	1:1	Co-crystal	Grinding liquid-assisted	• HSM: distinctive crystal habit from QUE and SA in mixing zone of photomicrographs • DTA: three endotherm peaks that similar with QUE and SA, with addition of new one at 280.32°C as a broad peak • PXRD: new peaks at six values of 2θ that differed from QUE & SA • FT-IR: shifted band at -OH group region to 3,411 cm^{-1}, decreased intensity of -OH region (observed as increased transmittance to 26%) • SEM: crystal habit of SA covered smaller crystals with different habit	Improved solubility (1.67 times higher) and dissolution rate (1.25 times higher) than pure QUE in citrate buffer (pH 5)	(Athiyah et al., 2019)

API	Co-former	Ratio	Type	Method	Characterizations	Advances	Ref
QUE	NM	1:1 1:2	Co-crystal	Solvent evaporation	• PXRD: unique patterns compared with pure QUE & NM • DSC: endothem peaks as cocrystalline melting point at 231.77°C and 195.1°C • FT-IR: shifted spectra in O-H (3,560-3,230), C=O (1,690-1,630), and N-H (3,520-3,350) vibrations of QUE-NM (1:1), as well as 1:2	Faster dissolution rate, supersaturated dissolution curve (higher solubility) and improved oral bioavailability compared with pure QUE	(Wu et al., 2020)
QUE	MA	1:2	Co-crystal	Solvent evaporation	• DTA: new endotherm peak at 277.9°C, presences of dehydration peak, decomposition of MA, and melting points of MA & QUE • PXRD: new diffraction peaks at three 2θ values • SEM: similar crystal shape as MA, covered with QUE crystal in uniform size • FT-IR: slightly shifted IR band of -OH to 3,418 cm^{-1}, and some differences with PM in C-O-C and aromatic group bands	Increased dissolution rate and %dissolution efficiency compared with pure QUE and PM	(Setyawan et al., 2018)
QUE	BYP	1:2	Co-crystal	Solvent evaporation	• SCXRD: asymmetric unit linked two molecules of QUE with two BYP through IV R_4^4 synthon (formed tetramer), tertramer further linked by interdimer H-bond (formed 2D layer), and 2D layers held by H-bonds & π-π stacking (formed 3D structure) • PXRD: different pattern from QUE & BYP dehydrate • ^{1}H-NMR & ^{13}C-NMR: confirmed the identity, purity, and BYP stoichiometric ratio	Efficacy of antibacterial inhibitory activity against *Staphylococcus aureus* and *Escherichia coli*	(Zhang et al., 2017a)
MYR	PRL	1:2	Co-crystal	Sonocrystallization	• ^{1}H-NMR: characteristic peaks area of MYR and PRL • DSC: single endotherm peak at 238.53°C which lower than pure MYR • FT-IR: appeared bands at 2,943, 1596, and 1,571 cm^{-1} which indicated as intermolecular H-bond from O-H and C=O groups of MYR with -COOH and -NH- groups of PRL • PXRD: new characteristic interference peaks at eight 2θ values • SEM: spherical particles (10 μm, which are smaller than MYR) with smooth surfaces	Increased solubility and dissolution rate which 7.69 higher than coarse MYR in 40 min; also occurrence of "spring and parachute" phenomenon	(Liu et al., 2016b)
MYR	BYP.H_2O	1:2	Co-crystal	Solvent evaporation	• SCXRD: asymmetric unit linked two molecules of MYR with 2 molecules of H_2O by VII R_6^6 synthon (formed tetramer), tertramer interconnected by three molecules of BYP (formed 2D layer), and 2D layers held by H-bonds & π-π stacking (formed 3D structure) • PXRD: different pattern from MYR & BYP dehydrate • ^{1}≈NMR & ^{13}C-NMR: confirmed the identity, purity, and BYP stoichiometric ratio	Efficacy of antibacterial inhibitory activity against *S. aureus* and *E. coli*	(Zhang et al., 2017a)

API	Co-former	Ratio	Type	Method	Characterizations	Advances	Ref
MYR	PRC	1:1	Co-crystal	Solvent evaporation, solvent-drop grinding	• SCXRD: orthorhombic system comprises neutral forms of heterodimer molecular assembled via H-bonds at H_{15}-O_{7A} and H_{7A1}-O_3. Heterodimers extended through H-O contacts into ribbons and interconnected with H-bonds (formed 2D), then PRC molecules interconnected by stacked manner and MYR linked to PRC by H-bonding (formed 3D) • FT-Raman: shifted into lower & higher frequencies of vibrational bands corresponding to OH groups • TG-DTA & DSC: single and sharp endotherm peak at 204.92°C, also confirmed unsolvated form • ^{1}H-NMR: confirmed identity, purity, and PRC stoichiometric ratio	Successful of MYR-PRC cocrystal using solvent-drop grinding method	(Sowa et al., 2014a)

Abbreviations: AA, ascorbic acid; β-CD, β-cyclodextrin; BBB, blood brain barrier; BYP, 4,4'-bipyridine; CA, cinnamic acid; CAF, caffeine; CD, cumulative dissolution; COOH, carboxylic acid; CS, complexation stoichiometry; CUR, *curcumin*; DSC, differential scanning calorimetry; DTA, differential thermal analysis; DX, dextrose; EC, electrostatic charge: FT-IR, Fourier transformation infrared; FT-Raman, Fourier transformation Raman; GEN, genistein; GIT, gastrointestinal tract; HP-β-CD, hydroxypropyl-β-cyclodextrin; HSM, hot stage microscopy; INM, isonicotinamide; MA, malonic acid; MYR, *myricetin*; NM, nicotinamide; NMR, nuclear magnetic resonance; PIP, *piperine*; PM, physical mixture; PRC, piracetam; PRL, proline; PXRD, powder X-ray diffraction; QUE, quercetin; RSV, resveratrol; SA, succinic acid; SAC, saccharine; SCXRD, single-crystal X-ray diffraction; SEM, scanning electron microscopy; Smax, maximum solubility; TG, thermogravimetry.

solvent evaporation or wet grinding methods (Pantwalawalkar et al., 2021). formulated CUR with ascorbic acid (AA) cocrystals using the solvent evaporation technique in 0.50-, 0.55-, 0.60-, and 0.65-mole fractions. AA was selected because of the presence of H-bonds between phenolic groups (-OH) in CUR and acidic hydrogens (-H) in AA. Based on the in-silico studies, AA has a high probability of cocrystallization, has sufficient structural similarity, exhibits synergistic biological activity, and presented van der Waal and hydrophobic interactions with CUR. The evaluation of the saturation solubility of CUR-AA indicated that the cocrystals were more soluble than CUR in distilled water (576-fold), buffer pH 1.2 (10-fold), and buffer pH 6.8 (9-fold), which was attributed to stronger molecular interactions, and consistently exhibited better solubility because of independent polymorphic transformations. The dissolution study of CUR-AA cocrystals revealed superior CUR dissolution compared with pure CUR and PM in the same medium as the solubility test (Pantwalawalkar et al., 2021).

In other research, Katherine et al. (2018) prepared CUR with dextrose (DX) cocrystals using the solvent evaporation method. Besides being proposed as GRAS and a widely available coformer, DX (or D-glucose) has five hydroxyl (-OH) groups as potential H-bonding sites. This H-bonding was suggested to prevent instability of CUR by stabilizing the lone pair electrons of oxygen in the β-diketone linker. Among all the considerations, the CUR-AA and CUR-DX crystallization phase was confirmed by related characterizations. Based on CUR content study, CUR-DX cocrystals showed slow and steady increases (from 0.18% to 0.29%) as the initial CUR concentration (from 0.2% to 1%), indicated that cocrystallization process was more efficient at a low concentration. This was strengthened by cocrystal solubility that increased to > 23,000 μg/mL (from 0.2% CUR concentration) that was hypothesized to be due to H-bonding between hydroxyl groups (from DX) with either carbonyl or phenolic groups (from CUR). Furthermore, in stability studies, CUR-DX was more stable in the pH range of 1–7 and presented a 33% decrease in absorbance at pH >7 (Katherine et al., 2018).

CUR cocrystals with resveratrol (RSV) in a 1:1 molar ratio were developed by Dal Magro et al. (2021) using cocrystallization with the supercritical solvent (CSS) technique. The selection of RSV and the formation of drug-drug cocrystals in this study were suggested to have a synergistic clinical effect with the enhancement of drug solubility through decreased lattice energy and improved affinity with the solvent. In addition, fast kinetics were reportedly because of ability of CSS to form cocrystals rapidly in a single step with less organic solvent used, which could reduce photodegradation of CUR and RSV. The lower lattice energy of cocrystals confirmed by DSC thermogram and PXRD diffractogram indicated that a weaker crystalline structure was formed with decreased particle size. Based on the solubility analysis, CUR-RSV cocrystals showed higher solubility of CUR and RSV in water, PBS (phosphate buffer solution), and 0.1 M HCl medium. The inference of

solubility and dissolution profile enhancement is influenced by reduction of solids interaction, weaker crystalline structure, smaller particle size, and higher coformer solubility (Dal Magro et al., 2021).

Furthermore, Rathi et al. (2019) developed cocrystal of CUR with cinnamic acid (CA) that formed in 0.3-mole fraction using solvent evaporation method. In this study, eutectics are formed in 0.15- and 0.33-mole fraction. This was confirmed with various characterizations that conclude as CUR-CA cocrystal formed by H-bond between carbonyl (C=O) of CA with phenolic (-OH) of CUR involved ι-ι stacking interactions. This answered the reason of selecting CA as coformer because of its similarity chemical structure with one half of basic CUR skeleton that suggested as potential H-bonds and molecular aggregate formation within the cocrystal component. Other than that, further studies to obtain a single crystal is necessary to lead advances of dissolution and other physicochemical studies of CUR-CA cocrystals (Rathi et al., 2019).

4.2 Semipolar Compounds

4.2.1 *Genistein* (GEN)

GEN is one of the most abundant isoflavonoids in soybeans, alfalfa and clover sprouts, broccoli, cauliflower, sunflower, and cumin (Jaiswal et al., 2019). GEN is also known has various bioactivities, such as antimicrobial (Choi et al., 2018), anticancer (Danciu et al., 2014), antioxidant (Braxas et al., 2019; Javanbakht et al., 2014), antidiabetic (Demir et al., 2019), and anti-inflammatory (Incir et al., 2016). However like other flavonoids, GEN also has similar weakness belongs to BCS class II which has very low water solubility (0.81 μg/mL) with high permeability (Sowa et al., 2014a), so pharmaceutical use of GEN is relatively limited. Several techniques also have been carried out to enhance GEN clinical use, including inclusion complexes (Daruházi et al., 2013), hydrogel matrix (Chen et al., 2013b), nano-formations (Aditya et al., 2013; Zhang et al., 2013), eutectic crystals (Buddhiranon and Kyu, 2012), and MCCs (Sowa et al., 2014b; Sowa et al., 2013b; Sowa et al., 2013a; Zhang et al., 2017a). Various GEN cocrystals reported by researchers which will be discussed (Table 1).

Currently, GEN-BYP cocrystals (1:1 molar ratio) are formulated with the solvent evaporation method. BYP was selected because of the presence of rigid linear structure with two terminal N atoms as potential sites for H-bonds (H-N) toward surface hydroxyls of GEN. The study confirmed the relation between the possible number of intermolecular H-bonds and stoichiometric ratio of cocrystals formed by the presence of two intermolecular H-bonds at H_7-N_4 and H_4-N_4 between GEN and BYP in cocrystals with 1:1 molar ratio (Figure 5). GEN-BYP cocrystals which exhibited lower melting point than GEN also formed a sheet via interchain H-bonds (H-O) between GEN molecules. The solubility study reveals cocrystals were more soluble than intact GEN, which determined by the higher maximum solubility (S_{max}) of cocrystals that reached after 130 min (while the GEN in 240 min) at concentration of 23.44 vs. 15.71 μg/mL. The result strengthened by the test of antibacterial activity which shows cocrystals more effective against bacteria than intact GEN (Zhang et al., 2017b).

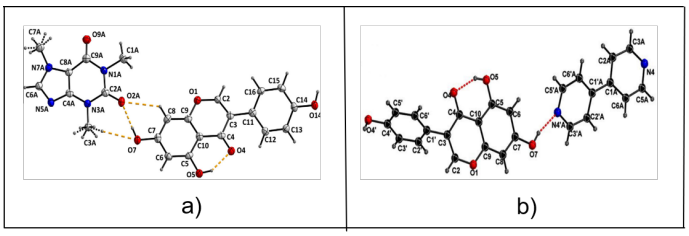

Figure 5. The intermolecular Reaction of GEN-CAF (a) and GEN-BYP (b). Reprinted with Permission of Ref (Sowa et al., 2014b; Zhang et al., 2017b). Copyright 2017 Elsevier B.V. for GEN-BYP and Copyright 2014 Elsevier B.V. for GEN-CAF

On the other hand, GEN cocrystals have been formulated with several coformers including caffeine (CAF), nicotinamide (NM), and isonicotinamide (INM) by (Sowa et al., 2014b; Sowa et al., 2013a;Sowa et al., 2013b). CAF was selected based on the chemical structure that contained 2 amide (-N-C=O) groups that suggested it would form H-bonds with 2 hydroxyls (-OH) groups of GEN (Figure 5). GEN-CAF (in 1:1 molar ratio) was prepared in 3 methods, including solvent-drop grinding with the addition of eight different solvents, solvent evaporation with EtOH, and slurrying technique with MetOH. The co-grinding GEN-CAF showed the occurrence of intermolecular H-bonding and the formation of the crystalline phase. The solubility study reveals that cocrystal was more soluble than intact GEN which was determined by the higher maximum solubility (S_{max}) of cocrystal reached 0.861 compared to 0.588 mg/mL. Cocrystal was also observed to be thermodynamically stable by PXRD analysis. The result explained the correlation of coformer solubilization and melting-point-solubility factors that might increase the solubility of API (Sowa et al., 2014b).

Previously, Sowa et al. (2013a) and Sowa et al. (2013b)) reported the analysis of GEN-INM cocrystallizations that build upon GEN-NM cocrystal application. Besides being included as GRAS and widely used for various carboxyl and hydroxyl-derived APIs, pyridine-derived (NM and INM) coformers were selected based on the recent study that stated H-N_{arom} heterosynthon could be the most competitive motif in crystallizing of phenolic compounds with pyridine-derived coformers. GEN-NM (1:1 molar ratio) cocrystal was prepared with solvent evaporation using EtOH-MetOH-H_2O (45:45:10 v/v/v) method and generated GEN-NM monohydrate. The water molecule plays an active role in generating 1-, 2-, 3-dimensional networks to form a sheet of GEN-NM by building H-bonds in OH-GEN and GEN-NM as inter-chains. The intra-chain formed NM-GEN-OH-NM-GEN-OH via H-bonding, and there were no homomolecular interactions observed. This has happened to GEN-INM which exhibited inter-and intra-chain by H-bonding without homomolecular interactions between GEN molecules. Distinct in the preparation, GEN-

INM (1:2 molar ratio) was prepared with solvent evaporation using propane-2-ol. In these studies, the authors successfully explained the application of pyridinecarboxamide coformers in flavonoid (GEN) cocrystallization (Sowa et al., 2013a; Sowa et al., 2013b). However, there was no evaluation process of physicochemical properties, such as solubility or dissolution studies, referring to advances in GEN bioavailability.

4.3 Polar Compounds

4.3.1 *Quercetin* (QUE)

QUE is a flavonoid in the flowers, leaves, and fruit of many plants, including *Sophora japonica*, *Dendranthema morifolium*, and *Crataegus pinnatifida Bunge* (Dian et al., 2014). QUE also has a broad range of pharmacological activities, including antidiabetic (Coballase-Urrutia et al., 2013; Lee et al., 2012; Nguyen et al., 2015), antioxidant (Coballase-Urrutia et al., 2013; Moretti et al., 2012), anti-inflammatory (Maciel et al., 2013), antimicrobial (Andrés et al., 2013; Božič et al., 2012), cardioprotective (Larson et al., 2012), hepatoprotective (Ying et al., 2013), anticancer (Martinez-Perez et al., 2014), and antiviral (Nguyen et al., 2012) effects. However, the clinical use of QUE is limited because of its extremely low solubility in water (0.3 µg/mL) (Setyawan et al., 2018), reducing its bioavailability (Dian et al., 2014). In addition, QUE reportedly has a very low oral absorption capacity (only 2%) and tends to be susceptible to metabolic conjugation (Athiyah et al., 2019) which might contribute to its low bioavailability. Several techniques for improving the solubility and stability of QUE, such as solid dispersions (Li et al., 2013; Setyawan et al., 2017), film dispersions (Dian et al., 2014), microparticles (Silva et al., 2013), nanoparticles (Lee et al., 2016; Pal et al., 2013), inclusion complexes (Aytac et al., 2016), emulsions (Chen et al., 2018), and MCCs (Athiyah et al., 2019; Setyawan et al., 2018). MCCs of QUE have been studied in various designs which will be discussed further (Table 1).

Cocrystals of QUE with SA were prepared in 1:1 molar ratio using the grinding liquid-assisted method to observe the enhancement of QUE solubility and dissolution rate (Athiyah et al., 2019). Apart from being classified as GRAS by the FDA, SA has potential H-bonding sites which are expected to be H-bond donors for two hydroxyls (-OH) groups in QUE with two carboxylic acids (-COOH) groups of SA. The result from FT-IR spectroscopy analysis strengthened the hydrogen bonding as the intermolecular reaction between QUE and SA, however the predicted structure does not consider H-bonding competition among other functional groups (Figure 6). QUE-SA cocrystals were formed incompletely and interaction only occurred at the interface. The solubility test of QUE-SA cocrystals was performed with spiked QUE standard solution, resulting in a slightly increased QUE concentration of cocrystal formation than QUE intact at 1.57±0.04 vs. 0.94±0.02 ($\times 10^{-4}$ w/v). The in vitro dissolution test also conducted based on the United States Pharmacopeia monograph indicated a 1.25 higher dissolution rate than that of intact QUE (Athiyah et al., 2019).

In addition, cocrystals of QUE were formulated with 4,4'-bipyridine (BYP) in a 1:2 molar ratio using the solvent evaporation method by (Zhang et al., 2017a). BYP was selected as the most used and readily available coformer that exhibited a rigid linear structure with terminal N atoms and a good π-electron conjugated system. QUE-BYP cocrystal was successfully formed and confirmed by various characterizations, which shows tetramer as a new crystalline phase through IV R_4^4 synthon (Figure 6), then tetramer further linked by interdimer H-bonds & π-π stacking to form two- and three-dimensional (2D and 3D) structures. The antimicrobial properties of QUE-BYP cocrystals were evaluated. The cocrystal had inhibitory activity against *Staphylococcus aureus* and *Escherichia coli*; however, this significant finding is not supported by any solubility or dissolution studies related to the enhancement of physicochemical properties (Zhang et al., 2017a). Furthermore, cocrystals of QUE with nicotinamide (NM) in 1:1 and 1:2 molar ratios were prepared by using the solvent evaporation method (Wu et al., 2020). NM has an amide group (HN-C=O) likely to serve as donors in H-bond formation with QUE. Moreover, Setyawan et al. (2018) described a cocrystal of QUE with malonic acid (MA) in a 1:2 molar ratio that was prepared by the solvent evaporation method. MA has two carboxylic acid (-COOH) groups that are suggested to form H-bonds with two hydroxyls (-OH) groups in QUE. The formation of QUE-NM and QUE-MA cocrystals was confirmed with several characterizations; the QUE-NM cocrystal (1:2) has a lower melting point than the 1:1 cocrystal and an indication of weak intermolecular reactions.

The *in vitro* dissolution test of QUE-NM was conducted in a pure water medium. The test showed significantly rapid dissolution and a supersaturated dissolution curve (higher solubility) of QUE-NM cocrystals. This plateaus at 4.5 µg/mL, which is three times higher than intact QUE after 6 hours. Moreover, the study effectively reported higher concentrations of QUE orally administered to rats, as shown in the in vivo pharmacokinetics study of QUE-NM (Wu et al., 2020). In addition, the dissolution profile showed a significantly increased % dissolved QUE in QUE-MA cocrystals that reached 95.30% vs. <65% in intact QUE at 60 min. Moreover, the %DE (dissolution effi-

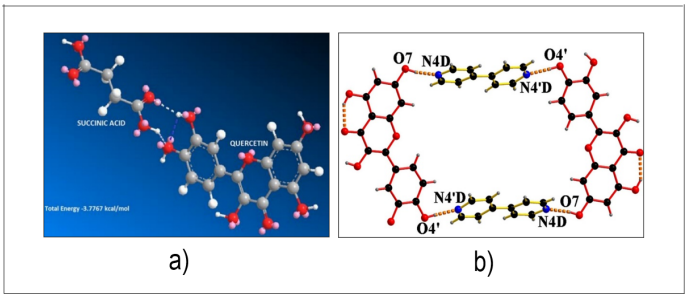

Figure 6. Intermolecular Reaction of QUE-SA (a) and QUE-BYP (b). Reprinted with Permission of Ref (Athiyah et al., 2019; Zhang et al., 2017a). Copyright 2016 Elsevier B.V. for figure QUE-BYP

ciency) of QUE-MA was 82.57±2.81%, which is higher than 64.46±0.93% in QUE (Setyawan et al., 2018).

4.3.2 *Myricetin* (MYR)

MYR is a flavonoid that was first identified in the Myricaceae family in *Comptonia peregrine* (*L.*) *Coult*, and *Morella cerifera* (*L.*). MYR has many clinical activities, including antioxidant (Barzegar, 2016; Guitard et al., 2016; Guo et al., 2016), anti-inflammatory (Sun et al., 2019), anticancer (Kim et al., 2014), antimicrobial (Wu et al., 2013), antidiabetic (Chen et al., 2016; Yang et al., 2019), immunomodulatory (Ghassemi-Rad et al., 2018), antiviral (Yu et al., 2012), and neuroprotective (Ma et al., 2015; Naldi et al., 2012; Ramezani et al., 2016; Ren et al., 2018) effects. However, MYR has limited water solubility (16.6 μg/mL) and low bioavailability, as seen in pre-clinical trials (9.62%) caused the clinical use of MYR to be limited (Dang et al., 2014; Sowa et al., 2014b). To maximize the potential of MYR, several approaches have been tested, such as microemulsions (Guo et al., 2016), nanoemulsions (Qian et al., 2017), micelles (Sun et al., 2019), inclusion complexes (Han et al., 2020), solid dispersions (Franklin and Myrdal, 2015), and the most widely developed MCCs (Liu et al., 2016a; Liu et al., 2016b; Sowa et al., 2014b; Zhai et al., 2016). Various cocrystals of MYR were formulated to overcome its physicochemical properties by crystal engineering (Table 1).

Cocrystals of MYR with proline (PRL) in 1:2 molar ratio were formulated using the sonocrystallization method (Liu et al., 2016b). The PRL was selected based on recent studies of amino acids that have carboxylic acid groups and amino acids that tend to form H-bonds with hydroxyl or carbonyl groups in MYR. MYR-PRL cocrystals were formed by intermolecular H-bond between MYR and PRL with lower melting points and smaller particle sizes that were confirmed by various characterizations. MYR-PRL cocrystals had a higher solubility and dissolution rate than coarse MYR, indicated by the peak solubility of cocrystals was 7.25 μg/mL (which is 7.69 higher) in 40 min. Moreover, the "spring and parachute" phenomenon was observed in the dissolution profile of MYR-PRL with the supersaturation of MYR (Liu et al., 2016a).

Furthermore, BYP dehydrates are also used as a coformer in formulating MYR-BYP-H_2O cocrystals (1:1 molar ratio) using the solvent evaporation method (Zhang et al., 2017a). MYR-BYP cocrystals were successfully formed with the involvement of H_2O molecules and confirmed by various characterizations, concluding as a new crystalline phase formed tetramer through VII R_6^6 synthon (Figure 7) and interconnected by H-bond & π-π stacking to form 3D structure. Conversely, Sowa et al. compared cocrystals of MYR with piracetam (PRC) in 1:1 molar ratio using two different methods (solvent evaporation and solvent-drop grinding) (Sowa et al., 2014a). The MYR-PRC cocrystals successfully resulted in a heterodimer that linked MYR and PRC by H-bonds, then formed 2D and 3D molecular structures by inter-ribbon interactions with H-bonds without homomolecular interactions of PRC molecules (Figure 7). The study concluded that solvent-drop grinding had

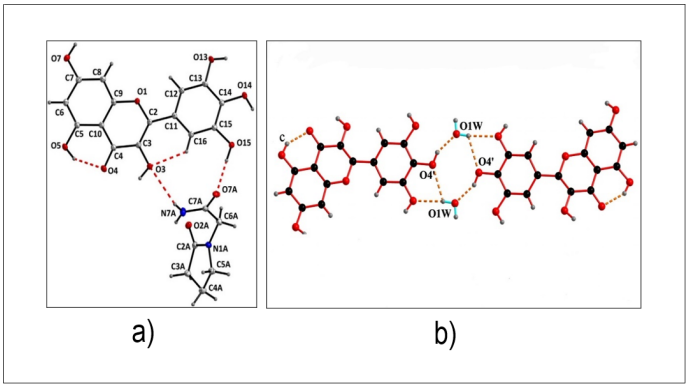

Figure 7. Intermolecular reaction of MYR-PRC (a) and MYR-BYP-H_2O (b). Reprinted with Permission of Ref (Sowa et al., 2014a; Zhang et al., 2017a). Copyright 2016 Elsevier B.V. for Figure QUE-BYP-H_2O; and Copyright 2013 Elsevier B.V. for MYR-

been proven to be a successful approach toward the synthesis of the MYR-PRC crystalline phase. Whereas MYR-BYP-H_2O cocrystals were evaluated for their antibacterial properties and the efficacy of the inhibitory activity against *S. aureus* and *E. coli* (Zhang et al., 2013). However, these significant findings are not supported by any solubility or dissolution studies related to the enhancement of physicochemical properties.

Studies have shown that different coformers and preparation methods provide different enhancements of physicochemical properties. An example of the intermolecular interactions formed between APIs and coformers is the formation of H-bonds between hydroxyl (-OH) functional groups in phenols, such as those in the polar phytochemicals QUE and MYR, with carboxylic acid (-COOH) functional groups in coformers. Amide (-NH-C=O) and N-heterocyclic functional groups also potentially interact intermolecularly and form H-bonds with phenols. Similarly, intermolecular interactions occurred between the phenolic functional group of GEN (a semipolar compound) and the carbonyl (-C=O) functional group of a coformer, which was potentially replaced by a coformer with an N-heterocyclic functional group. Furthermore, the carbonyl functional groups in nonpolar phytochemicals like PIP and CUR are most likely to form H-bonds with carboxylic acid, amide, and phenolic functional groups.

The preparation methods should be an important consideration in the formation of MCCs using specific APIs, however there is a lack of variety in the methods for current phytochemical MCCs preparation. The phytochemicals that form MCCs with more soluble coformers are most likely prepared using conventional techniques, such as wet or liquid-assisted grinding, solvent evaporation, or slurrying, whereas these techniques are less effective when performed on less soluble coformers. For instance, there are less soluble APIs that, when paired with less soluble APIs as coformers, form a drug-drug type of MCC. This type of crystal is effectively formed with high-

performance methods, such as supercritical fluid processing and sonocrystallization.

The type of MCC formed is also a factor that must be considered when optimizing the enhancement of physicochemical properties. This review shows that PIP in the form of a salt is more soluble than a cocrystal and inclusion complex, whereas the cocrystal form is more stable because of higher crystallinity. This also applies to other APIs that primarily form cocrystals, as seen when reviewing the literature. Therefore, many researchers seek to form salt-type MCCs. Nevertheless, APIs that can form salt-type MCCs are lacking, causing the cocrystal-type to be also widely preferred which has better crystallinity and stability over the other types of MCCs.

5. CONCLUSIONS

Studies show that crystal engineering through the formation of MCCs enhances phytochemical physicochemical properties, including solubility, dissolution rate, stability, and permeability. More studies about other physicochemical properties, including stability, permeability, and compressibility, could provide a better understanding of clinical and industrial applications. However, because very few reports of pharmaceutical crystal engineering for phytochemicals in the selection of coformers, methods of preparation, and further design of MCCs exist, these topics must necessarily be explored. Therefore, this study led to the understanding that much remains to be developed in MCC engineering, including identifying more specific coformers for currently available phytochemicals, revealing more improvements to physicochemical properties of discovered phytochemical MCCs, and exploring the pattern of this approach. Furthermore, crystal engineering manifests as a significant opportunity for increasing the use of phytochemicals in the pharmaceutical industry.

6. ACKNOWLEDGMENT

The authors sincerely acknowledge the Directorate of Higher Degrees of Indonesia for granting this research under the scheme Basic Research (number 011/E5/PG.02.00.PT/2022).The authors would also express kind gratitude to all the authors of the publications, patents, and other contents used in the writing of this paper.

7. AUTHORS CONTRIBUTIONS

Conceptualization, E.Z; writing–original draft, D.S.L; writing–review & editing, L.F, M.T, E.Z, and D.S.L; supervision, E.Z; funding acquisition, E.Z. All authors have read and agreed to the published version of the manuscript.

8. CONFLICT OF INTEREST

The authors declare no conflict of interest.

REFERENCES

Aditya, N., M. Shim, I. Lee, Y. Lee, M. H. Im, and S. Ko (2013). Curcumin and Genistein Coloaded Nanostructured Lipid Carriers: in Vitro Digestion and Antiprostate Cancer Activity. *Journal of Agricultural and Food Chemistry*, **61**(8); 1878–1883

Al-Dulaimi, A. F., M. Al-kotaji, and F. T. Abachi (2022). Co-Crystals For Improving Solubility And Bioavailability of Pharmaceutical Products. *Egyptian Journal of Chemistry*, **65**(1); 81–89

Alippilakkotte, S. and L. Sreejith (2018). Pectin Mediated Synthesis of Curcumin Loaded Poly (Lactic Acid) Nanocapsules for Cancer Treatment. *Journal of Drug Delivery Science and Technology*, **48**; 66–74

Andrés, S., M. L. Tejido, R. Bodas, L. Morán, N. Prieto, C. Blanco, and F. J. Giráldez (2013). Quercetin Dietary Supplementation of Fattening Lambs at 0.2% Rate Reduces Discolouration and Microbial Growth in Meat During Refrigerated Storage. *Meat Science*, **93**(2); 207–212

Athiyah, U., P. A. Kusuma, T. Tutik, M. L. Lestari, D. Isadiartuti, D. P. Paramita, and D. Setyawan (2019). Crystal Engineering of Quercetin by Liquid Assisted Grinding Method. *Jurnal Teknologi*, **81**(1); 39–45

Aytac, Z., S. I. Kusku, E. Durgun, and T. Uyar (2016). Quercetin/β-Cyclodextrin Inclusion Complex Embedded Nanofibres: Slow Release and High Solubility. *Food Chemistry*, **197**; 864–871

B. Arnao, M. and J. Hernández-Ruiz (2018). The Potential of Phytomelatonin as a Nutraceutical. *Molecules*, **23**(1); 238

Balan, P., G. Mal, S. Das, and H. Singh (2016). Synergistic and Additive Antimicrobial Activities of Curcumin, Manuka Honey and Whey Proteins. *Journal of Food Biochemistry*, **40**(5); 647–654

Barzegar, A. (2016). Antioxidant Activity of Polyphenolic Myricetin in Vitro Cell-Free and Cell-Based Systems. *Molecular Biology Research Communications*, **5**(2); 87

Batisai, E. (2021). Solubility Enhancement of Antidiabetic Drugs Using a Co-Crystallization Approach. *Chemistry Open*, **10**(12); 1260–1268

Bhalekar, M. R., A. R. Madgulkar, P. S. Desale, and G. Marium (2017). Formulation of Piperine Solid Lipid Nanoparticles (SLN) for Treatment of Rheumatoid Arthritis. *Drug Development and Industrial Pharmacy*, **43**(6); 1003–1010

Boksa, K., A. Otte, and R. Pinal (2014). Matrix Assisted Cocrystallization (MAC) Simultaneous Production and Formulation of Pharmaceutical Cocrystals by Hot Melt Extrusion. *Journal of Pharmaceutical Sciences*, **103**(9); 2904–2910

Božič, M., S. Gorgieva, and V. Kokol (2012). Homogeneous and Heterogeneous Methods for Laccase Mediated Functionalization of Chitosan by Tannic Acid and Quercetin. *Carbohydrate Polymers*, **89**(3); 854–864

Braxas, H., M. Rafraf, S. K. Hasanabad, and M. A. Jafarabadi (2019). Effectiveness of Genistein Supplementation on Metabolic Factors and Antioxidant Status in Postmenopausal Women with Type 2 Diabetes Mellitus. *Canadian Journal of Diabetes*, **43**(7); 490–497

Buddhiranon, S. and T. Kyu (2012). Solubilization of Genistein in Poly (Oxyethylene) Through Eutectic Crystal Melt-

ing. *The Journal of Physical Chemistry B*, **116**(27); 7795–7802
Chen, C. Y., W. Li, K. P. Qu, and C. R. Chen (2013a). Piperine Exerts Anti Seizure Effects via the TRPV1 Receptor in Mice. *European Journal of Pharmacology*, **714**(1-3); 288–294
Chen, F., J. Peng, D. Lei, J. Liu, and G. Zhao (2013b). Optimization of Genistein Solubilization by κ-Carrageenan Hydrogel Using Response Surface Methodology. *Food Science and Human Wellness*, **2**(4); 124–131
Chen, J., Y. Wu, J. Zou, and K. Gao (2016). α-Glucosidase Inhibition and Antihyperglycemic Activity of Flavonoids from Ampelopsis Grossedentata and The Flavonoid Derivatives. *Bioorganic & Medicinal Chemistry*, **24**(7); 1488–1494
Chen, X., D. J. McClements, Y. Zhu, Y. Chen, L. Zou, W. Liu, C. Cheng, D. Fu, and C. Liu (2018). Enhancement of The Solubility, Stability and Bioaccessibility of Quercetin Using Protein Based Excipient Emulsions. *Food Research International*, **114**; 30–37
Choi, H., J. S. Park, K. M. Kim, M. Kim, K. W. Ko, C. G. Hyun, J. W. Ahn, J. H. Seo, and S. Y. Kim (2018). Enhancing The Antimicrobial Effect of Genistein by Biotransformation in Microbial System. *Journal of Industrial and Engineering Chemistry*, **63**; 255–261
Clarke, H. D. (2012). *Crystal Engineering of Multi-Component Crystal Forms: The Opportunities and Challenges in Design*. University of South Florida
Coballase-Urrutia, E., J. Pedraza-Chaverri, N. Cárdenas-Rodríguez, B. Huerta-Gertrudis, M. E. García-Cruz, H. Montesinos-Correa, D. J. Sánchez-González, R. Camacho-Carranza, and J. J. Espinosa-Aguirre (2013). Acetonic and Methanolic Extracts of Heterotheca Inuloides, and Quercetin, Decrease CCl_4 Oxidative Stress in Several Rat Tissues. *Evidence-Based Complementary and Alternative Medicine*, **2013**; 1–13
Da Cruz, G. M. P., C. F. B. Felipe, F. A. Scorza, M. A. C. da Costa, A. F. Tavares, M. L. F. Menezes, G. M. de Andrade, L. K. A. Leal, G. A. C. Brito, and M. da Graça Naffah-Mazzacoratti (2013). Piperine Decreases Pilocarpine Induced Convulsions by GABAergic Mechanisms. *Pharmacology Biochemistry and Behavior*, **104**; 144–153
Dal Magro, C., A. E. dos Santos, M. M. Ribas, G. P. Aguiar, C. R. Volfe, M. L. Lopes, A. M. Siebel, L. G. Müller, A. J. Bortoluzzi, and M. Lanza (2021). Production of Curcumin Resveratrol Cocrystal Using Cocrystallization with Supercritical Solvent. *The Journal of Supercritical Fluids*, **171**; 105190
Danciu, C., C. Soica, M. Oltean, S. Avram, F. Borcan, E. Csanyi, R. Ambrus, I. Zupko, D. Muntean, and C. A. Dehelean (2014). Genistein in 1: 1 inclusion Complexes with Ramified Cyclodextrins: Theoretical, Physicochemical and Biological Evaluation. *International Journal of Molecular Sciences*, **15**(2); 1962–1982
Dang, Y., G. Lin, Y. Xie, J. Duan, P. Ma, G. Li, and G. Ji (2014). Quantitative Determination of Myricetin in Rat Plasma by Ultra Performance Liquid Chromatography Tandem Mass Spectrometry and its Absolute Bioavailability. *Drug Research*, **64**(10); 516–522
Daruházi, Á. E., T. Kiss, M. Vecsernyés, L. Szente, É. Szőke, and É. Lemberkovics (2013). Investigation of Transport of Genistein, Daidzein and Their Inclusion Complexes Prepared with Different Cyclodextrins on Caco-2 Cell Line. *Journal of Pharmaceutical and Biomedical Analysis*, **84**; 112–116
Demir, Y., L. Durmaz, P. Taslimi, and İ. Gulçin (2019). Antidiabetic Properties of Dietary Phenolic Compounds: Inhibition Effects on α-Amylase, Aldose Reductase, and α-Glycosidase. *Biotechnology and Applied Biochemistry*, **66**(5); 781–786
Dian, L., E. Yu, X. Chen, X. Wen, Z. Zhang, L. Qin, Q. Wang, G. Li, and C. Wu (2014). Enhancing Oral Bioavailability of Quercetin Using Novel Soluplus Polymeric Micelles. *Nanoscale Research Letters*, **9**(1); 1–11
Egbuna, C., J. C. Ifemeje, S. C. Udedi, S. Kumar, and C. Press (2019). *Phytochemistry: Fundamentals, Modern Techniques and Applications*. CRC Press Taylor & Francis Group
Ezawa, T., Y. Inoue, S. Tunvichien, R. Suzuki, and I. Kanamoto (2016). Changes in The Physicochemical Properties of Piperine β-Cyclodextrin Due to The Formation of Inclusion Complexes. *International Journal of Medicinal Chemistry*, **2016**; 1–9.
Franklin, S. J. and P. B. Myrdal (2015). Solid State and Solution Characterization of Myricetin. *AAPS PharmSciTech*, **16**(6); 1400–1408
Gadade, D. D. and S. S. Pekamwar (2016). Pharmaceutical Cocrystals: Regulatory and Strategic Aspects, Design and Development. *Advanced Pharmaceutical Bulletin*, **6**(4); 479
Gajda, M., K. P. Nartowski, J. Pluta, and B. Karolewicz (2019). Continuous, One Step Synthesis of Pharmaceutical Cocrystals via Hot Melt Extrusion from Neat to Matrix Assisted Processing State of the Art. *International Journal of Pharmaceutics*, **558**; 426–440
Ghassemi-Rad, J., M. Maleki, A. F. Knickle, and D. W. Hoskin (2018). Myricetin Induced Oxidative Stress Suppresses Murine T Lymphocyte Activation. *Cell Biology International*, **42**(8); 1069–1075
Gorgani, L., M. Mohammadi, G. D. Najafpour, and M. Nikzad (2017). Piperine The Bioactive Compound of Black Pepper: from Isolation to Medicinal Formulations. *Comprehensive Reviews in Food Science and Food Safety*, **16**(1); 124–140
Guitard, R., J. F. Paul, V. Nardello-Rataj, and J. M. Aubry (2016). Myricetin, Rosmarinic and Carnosic Acids as Superior Natural Antioxidant Alternatives to α-Tocopherol for The Preservation of Omega-3 Oils. *Food Chemistry*, **213**; 284–295
Guo, R. X., X. Fu, J. Chen, L. Zhou, and G. Chen (2016). Preparation and Characterization of Microemulsions of Myricetin for Improving its Antiproliferative and Antioxidative Activities and Oral Bioavailability. *Journal of Agricultural and Food Chemistry*, **64**(32); 6286–6294
Hadi, K. (2015). Spray Drying of Cocrystals for Engineering Particle Properties: Diploma Work
Han, D., Z. Han, L. Liu, Y. Wang, S. Xin, H. Zhang, and

Z. Yu (2020). Solubility Enhancement of Myricetin by Inclusion Complexation with Heptakis-O-(2-hydroxypropyl)-β-Cyclodextrin: A Joint Experimental and Theoretical Study. *International Journal of Molecular Sciences*, **21**(3); 766

Hasan, M., N. Belhaj, H. Benachour, M. Barberi-Heyob, C. Kahn, E. Jabbari, M. Linder, and E. Arab-Tehrany (2014). Liposome Encapsulation of Curcumin: Physico Chemical Characterizations and Effects on MCF7 Cancer Cell Proliferation. *International Journal of Pharmaceutics*, **461**(1-2); 519–528

Incir, S., I. M. Bolayirli, O. Inan, M. S. Aydın, I. A. Bilgin, I. Sayan, M. Esrefoglu, and A. Seven (2016). The Effects of Genistein Supplementation on Fructose Induced Insulin Resistance, Oxidative Stress and Inflammation. *Life Sciences*, **158**; 57–62

Jäger, R., R. P. Lowery, A. V. Calvanese, J. M. Joy, M. Purpura, and J. M. Wilson (2014). Comparative Absorption of Curcumin Formulations. *Nutrition Journal*, **13**(1); 1–8

Jaiswal, N., J. Akhtar, S. P. Singh, F. Ahsan, et al. (2019). An Overview on Genistein and its Various Formulations. *Drug Research*, **69**(06); 305–313

Javanbakht, M. H., R. Sadria, M. Djalali, H. Derakhshanian, P. Hosseinzadeh, M. Zarei, G. Azizi, R. Sedaghat, and A. Mirshafiey (2014). Soy Protein and Genistein Improves Renal Antioxidant Status in Experimental Nephrotic Syndrome. *Nefrologia*, **34**(4); 483–490

Jessica, A., R. Naura, U. Hasanah, E. Zaini, and L. Fitriani (2021). Pembentukan Multikomponen Kristal Piperin dan Kuersetin. *JOPS (Journal Of Pharmacy and Science)*, **4**(2); 1–11 (in Indonesia)

Jiao, D., J. Wang, W. Lu, X. Tang, J. Chen, H. Mou, and Q. Y. Chen (2016). Curcumin Inhibited HGF Induced EMT and Angiogenesis Through Regulating c-Met Dependent PI3K/Akt/mTOR Signaling Pathways in Lung Cancer. *Molecular Therapy-Oncolytics*, **3**; 16018

Kantatasiri, P. (2012). Future of Functional Foods and Nutraceutical Products: The Challenge and Potential of Thailand to ASEAN. *GMSARN International Journal*, **6**(3); 87–96

Karagianni, A., M. Malamatari, and K. Kachrimanis (2018). Pharmaceutical Cocrystals: New Solid Phase Modification Approaches for the Formulation of APIs. *Pharmaceutics*, **10**(1); 18

Katherine, D. Nugroho, and A. K. Sugih (2018). Preparation and Characterization of Highly Water Soluble Curcumin Dextrose Cocrystal. *The Journal of Pure and Applied Chemistry Research*, **7**(2); 140–148

Kharbanda, C., M. S. Alam, H. Hamid, K. Javed, S. Bano, Y. Ali, A. Dhulap, P. Alam, and M. Q. Pasha (2016). Novel Piperine Derivatives with Antidiabetic Effect as PPAR-γ Agonists. *Chemical Biology & Drug Design*, **88**(3); 354–362

Kim, M. E., T. K. Ha, J. H. Yoon, and J. S. Lee (2014). Myricetin Induces Cell Death of Human Colon Cancer Cells via BAX/BCL2 Dependent Pathway. *Anticancer Research*, **34**(2); 701–706

Kumar, S. (2018). Pharmaceutical Cocrystals: an Overview. *Indian Journal of Pharmaceutical Sciences*, **79**(6); 858–871

Larson, A. J., J. D. Symons, and T. Jalili (2012). Therapeutic Potential of Quercetin to Decrease Blood Pressure: Review of Efficacy and Mechanisms. *Advances in Nutrition*, **3**(1); 39–46

Lee, G. H., S. J. Lee, S. W. Jeong, H. C. Kim, G. Y. Park, S. G. Lee, and J. H. Choi (2016). Antioxidative and Antiinflammatory Activities of Quercetin Loaded Silica Nanoparticles. *Colloids and Surfaces B: Biointerfaces*, **143**; 511–517

Lee, S. Y., K. H. Kim, I. K. Lee, K. H. Lee, S. U. Choi, and K. R. Lee (2012). A New Flavonol Glycoside from Hylomecon Vernalis. *Archives of Pharmacal Research*, **35**(3); 415–421

Li, B., S. Konecke, K. Harich, L. Wegiel, L. S. Taylor, and K. J. Edgar (2013). Solid Dispersion of Quercetin in Cellulose Derivative Matrices Influences Both Solubility and Stability. *Carbohydrate Polymers*, **92**(2); 2033–2040

Liu, M., C. Hong, G. Li, P. Ma, and Y. Xie (2016a). The Generation of Myricetin Nicotinamide Nanococrystals by Top Down and Bottom Up Technologies. *Nanotechnology*, **27**(39); 395601

Liu, M., C. Hong, Y. Yao, H. Shen, G. Ji, G. Li, and Y. Xie (2016b). Development of a Pharmaceutical Cocrystal with Solution Crystallization Technology: Preparation, Characterization, and Evaluation of Myricetin Proline Cocrystals. *European Journal of Pharmaceutics and Biopharmaceutics*, **107**; 151–159

Lombard, J., D. A. Haynes, and T. le Roex (2020). Assessment of Co Sublimation for The Formation of Multicomponent Crystals. *Crystal Growth & Design*, **20**(12); 7840–7849

Ma, Z., G. Wang, L. Cui, and Q. Wang (2015). Myricetin Attenuates Depressant Like Behavior in Mice Subjected to Repeated Restraint Stress. *International Journal of Molecular Sciences*, **16**(12); 28377–28385

Maciel, R., M. Costa, D. Martins, R. Franca, R. Schmatz, D. Graça, M. Duarte, C. Danesi, C. Mazzanti, and M. Schetinger (2013). Antioxidant and Anti Inflammatory Effects of Quercetin in Functional and Morphological Aterations in Streptozotocin Induced Diabetic Rats. *Research in Veterinary Science*, **95**(2); 389–397

Maeno, Y., T. Fukami, M. Kawahata, K. Yamaguchi, T. Tagami, T. Ozeki, T. Suzuki, and K. Tomono (2014). Novel Pharmaceutical Cocrystal Consisting of Paracetamol and Trimethylglycine, a New Promising Cocrystal Former. *International Journal of Pharmaceutics*, **473**(1-2); 179–186

Malik, P., R. Ameta, and M. Singh (2014). Preparation and Characterization of Bionanoemulsions for Improving and Modulating the Antioxidant Efficacy of Natural Phenolic Antioxidant Curcumin. *Chemico-Biological Interactions*, **222**; 77–86

Mao, Q. Q., Z. Huang, X. M. Zhong, Y. F. Xian, and S. P. Ip (2014). Brain Derived Neurotrophic Factor Signalling Mediates the Antidepressant Like Effect of Piperine in Chronically Stressed Mice. *Behavioural Brain Research*, **261**; 140–145

Martinez-Perez, C., C. Ward, G. Cook, P. Mullen, D. McPhail, D. J. Harrison, and S. P. Langdon (2014). Novel Flavonoids

as Anti Cancer Agents: Mechanisms of Action and Promise for Their Potential Application in Breast Cancer. *Biochemical Society Transactions*, **42**(4); 1017–1023

McClements, D. (2012). Requirements for Food Ingredient and Nutraceutical Delivery Systems. In *Encapsulation Technologies and Delivery Systems for Food Ingredients and Nutraceuticals*. Elsevier; 3–18

Moretti, E., L. Mazzi, G. Terzuoli, C. Bonechi, F. Iacoponi, S. Martini, C. Rossi, and G. Collodel (2012). Effect of Quercetin, Rutin, Naringenin and Epicatechin on Lipid Peroxidation Induced in Human Sperm. *Reproductive Toxicology*, **34**(4); 651–657

Naldi, M., J. Fiori, M. Pistolozzi, A. F. Drake, C. Bertucci, R. Wu, K. Mlynarczyk, S. Filipek, A. De Simone, and V. Andrisano (2012). Amyloid β Peptide 25–35 Self Assembly and its Inhibition: a Model Undecapeptide System to Gain Atomistic and Secondary Structure Details of The Alzheimer's Disease Process and Treatment. *ACS Chemical Neuroscience*, **3**(11); 952–962

Nascimento, A. L., R. P. Fernandes, M. D. Charpentier, J. H. ter Horst, F. J. Caires, and M. Chorilli (2021). Co-Crystals of Non Steroidal Anti Inflammatory Drugs (NSAIDs): Insight Toward Formation, Methods, and Drug Enhancement. *Particuology*, **58**; 227–241

Nguyen, T. T. H., H. J. Woo, H. K. Kang, V. D. Nguyen, Y. M. Kim, D. W. Kim, S. A. Ahn, Y. Xia, and D. Kim (2012). Flavonoid Mediated Inhibition of SARS Coronavirus 3C Like Protease Expressed in Pichia Pastoris. *Biotechnology Letters*, **34**(5); 831–838

Nguyen, T. T. H., S. H. Yu, J. Kim, E. An, K. Hwang, J. S. Park, and D. Kim (2015). Enhancement of Quercetin Water Solubility with Steviol Glucosides and The Studies of Biological Properties. *Functional Foods in Health and Disease*, **5**(12); 437–449

Nwosu, O. K. and K. I. Ubaoji (2020). Nutraceuticals: History, Classification and Market Demand. In *Functional Foods and Nutraceuticals*. Springer; 13–22

Ouyang, D. y., L. H. Zeng, H. Pan, L. H. Xu, Y. Wang, K. P. Liu, and X. H. He (2013). Piperine Inhibits the Proliferation of Human Prostate Cancer Cells via Induction of Cell Cycle Arrest and Autophagy. *Food and Chemical Toxicology*, **60**; 424–430

Pachauri, M., E. D. Gupta, and P. C. Ghosh (2015). Piperine Loaded PEG-PLGA Nanoparticles: Preparation, Characterization and Targeted Delivery for Adjuvant Breast Cancer Chemotherapy. *Journal of Drug Delivery Science and Technology*, **29**; 269–282

Pal, R., S. Panigrahi, D. Bhattacharyya, and A. S. Chakraborti (2013). Characterization of Citrate Capped Gold Nanoparticl Equercetin Complex: Experimental and Quantum Chemical Approach. *Journal of Molecular Structure*, **1046**; 153–163

Pan, K., Q. Zhong, and S. J. Baek (2013). Enhanced Dispersibility and Bioactivity of Curcumin by Encapsulation in Casein Nanocapsules. *Journal of Agricultural and Food Chemistry*, **61**(25); 6036–6043

Pandit, R. S., S. C. Gaikwad, G. A. Agarkar, A. K. Gade, and M. Rai (2015). Curcumin Nanoparticles: Physico-Chemical Fabrication and its in Vitro Efficacy Against Human Pathogens. *3 Biotech*, **5**(6); 991–997

Pang, W., Y. Wu, N. Xue, Y. Li, S. Du, B. He, C. Yang, J. Wang, and Y. Zeng (2019). Retracted: Cocrystals of Curcumin-Isonicotinamide and Curcumin-Gallic Acid: Does The Weak Forces in Cocrystals Effect on Binding Profiles with BSA and Cell Cytotoxicity?

Pantwalawalkar, J., H. More, D. Bhange, U. Patil, and N. Jadhav (2021). Novel Curcumin Ascorbic Acid Cocrystal for Improved Solubility. *Journal of Drug Delivery Science and Technology*, **61**; 102233

Qian, J., H. Meng, L. Xin, M. Xia, H. Shen, G. Li, and Y. Xie (2017). Self Nanoemulsifying Drug Delivery Systems of Myricetin: Formulation Development, Characterization, and in Vitro and in Vivo Evaluation. *Colloids and Surfaces B: Biointerfaces*, **160**; 101–109

Quilaqueo, M., S. Millao, I. Luzardo-Ocampo, R. Campos-Vega, F. Acevedo, C. Shene, and M. Rubilar (2019). Inclusion of Piperine in β Cyclodextrin Complexes Improves Their Bioaccessibility and in Vitro Antioxidant Capacity. *Food Hydrocolloids*, **91**; 143–152

Quiñones, J. P., H. Peniche, and C. Peniche (2018). Chitosan Based Self Assembled Nanoparticles in Drug Delivery. *Polymers*, **10**(3); 235

Ramezani, M., N. Darbandi, F. Khodagholi, and A. Hashemi (2016). Myricetin Protects Hippocampal CA3 Pyramidal Neurons and Improves Learning and Memory Impairments in Rats with Alzheimer's Disease. *Neural Regeneration Research*, **11**(12); 1976

Rao, R. V., O. Descamps, V. John, and D. E. Bredesen (2012). Ayurvedic Medicinal Plants for Alzheimer's Disease: a Review. *Alzheimer's Research & Therapy*, **4**(3); 1–9

Rathi, N., A. Paradkar, and V. G. Gaikar (2019). Polymorphs of Curcumin and its Cocrystals with Cinnamic Acid. *Journal of Pharmaceutical Sciences*, **108**(8); 2505–2516

Raza, S. A., U. Schacht, V. Svoboda, D. P. Edwards, A. J. Florence, C. R. Pulham, J. Sefcik, and I. D. Oswald (2018). Rapid Continuous Antisolvent Crystallization of Multicomponent Systems. *Crystal Growth & Design*, **18**(1); 210–218

Ren, T., M. Hu, Y. Cheng, T. L. Shek, M. Xiao, N. J. Ho, C. Zhang, S. S. Y. Leung, and Z. Zuo (2019). Piperine Loaded Nanoparticles with Enhanced Dissolution and Oral Bioavailability for Epilepsy Control. *European Journal of Pharmaceutical Sciences*, **137**; 104988

Ren, Z., P. Yan, L. Zhu, H. Yang, Y. Zhao, B. P. Kirby, J. L. Waddington, and X. Zhen (2018). Dihydromyricetin Exerts a Rapid Antidepressant Like Effect in Association with Enhancement of BDNF Expression and Inhibition of Neuroinflammation. *Psychopharmacology*, **235**(1); 233–244

Ribas, M. M., G. P. S. Aguiar, L. G. Muller, A. M. Siebel, M. Lanza, and J. V. Oliveira (2019). Curcumin Nicotinamide Cocrystallization with Supercritical Solvent (CSS):

Synthesis, Characterization and in Vivo Antinociceptive and Anti Inflammatory Activities. *Industrial Crops and Products*, **139**; 111537

Roy, L., M. Lipert, and N. Rodriguez-Hornedo (2012). Cocrystal Solubility and Thermodynamic Stability. *Pharmaceutical Salts and Co-crystals*; 247–279

Salama, S. M., M. A. Abdulla, A. S. AlRashdi, S. Ismail, S. S. Alkiyumi, and S. Golbabapour (2013). Hepatoprotective Effect of Ethanolic Extract of *Curcuma Longa* on Thioacetamide Induced Liver Cirrhosis in Rats. *BMC Complementary and Alternative Medicine*, **13**(1); 1–17

Salsabila, H., L. Fitriani, and E. Zaini (2021). Recent Strategies for Improving Solubility and Oral Bioavailability of Piperine. *Int. J. Appl. Pharm*, **13**(4); 31–39

Sathisaran, I. and S. V. Dalvi (2017). Crystal Engineering of Curcumin with Salicylic Acid and Hydroxyquinol as Coformers. *Crystal Growth & Design*, **17**(7); 3974–3988

Savjani, J. K. (2015). Coâ€ Crystallization: An Approach to Improve the Performance Characteristics of Active Pharmaceutical Ingredients. *Asian Journal of Pharmaceutics (AJP)*, **9**(3); 147–151

Seo, J. A., B. Kim, D. N. Dhanasekaran, B. K. Tsang, and Y. S. Song (2016). Curcumin Induces Apoptosis by Inhibiting Sarco/Endoplasmic Reticulum Ca^{2+} ATPase activity in Ovarian Cancer Cells. *Cancer Letters*, **371**(1); 30–37

Setyawan, D., A. A. Fadhil, D. Juwita, H. Yusuf, and R. Sari (2017). Enhancement of Solubility and Dissolution Rate of Quercetin with Solid Dispersion System Formation Using Hydroxypropyl Methyl Cellulose Matrix. *Thai Journal of Pharmaceutical Sciences*, **41**(3); 112–116

Setyawan, D., S. A. Permata, A. Zainul, and M. L. A. D. Lestari (2018). Improvement in Vitro Dissolution Rate of Quercetin Using Cocrystallization of Quercetin Malonic Acid. *Indonesian Journal of Chemistry*, **18**(3); 531–536

Silva, L. F. C., G. Kasten, C. E. M. de Campos, A. L. Chinelatto, and E. Lemos-Senna (2013). Preparation and Characterization of Quercetin Loaded Solid Lipid Microparticles for Pulmonary Delivery. *Powder Technology*, **239**; 183–192

Sowa, M., K. Ślepokura, and E. Matczak-Jon (2013a). A 1: 2 Cocrystal of Genistein with Isonicotinamide: Crystal Structure and Hirshfeld Surface Analysis. *Acta Crystallographica Section C: Crystal Structure Communications*, **69**(11); 1267–1272

Sowa, M., K. Ślepokura, and E. Matczak-Jon (2013b). Cocrystals of Fisetin, Luteolin and Genistein with Pyridinecarboxamide Coformers: Crystal Structures, Analysis of Intermolecular Interactions, Spectral and Thermal Characterization. *CrystEngComm*, **15**(38); 7696–7708

Sowa, M., K. Ślepokura, and E. Matczak-Jon (2014a). A 1: 1 Pharmaceutical Cocrystal of Myricetin in Combination with Uncommon Piracetam Conformer: X-Ray Single Crystal Analysis and Mechanochemical Synthesis. *Journal of Molecular Structure*, **1058**; 114–121

Sowa, M., K. Ślepokura, and E. Matczak-Jon (2014b). Solid State Characterization and Solubility of a Genistein Caffeine Cocrystal. *Journal of Molecular Structure*, **1076**; 80–88

Stasiłowicz, A., N. Rosiak, E. Tykarska, M. Kozak, J. Jenczyk, P. Szulc, J. Kobus-Cisowska, K. Lewandowska, A. Płazińska, and W. Płaziński (2021). Combinations of Piperine with Hydroxypropyl-β-Cyclodextrin as a Multifunctional System. *International Journal of Molecular Sciences*, **22**(8); 4195

Sun, F., Z. Zheng, J. Lan, X. Li, M. Li, K. Song, and X. Wu (2019). New Micelle Myricetin Formulation for Ocular Delivery: Improved Stability, Solubility, and Ocular Anti Inflammatory Treatment. *Drug Delivery*, **26**(1); 575–585

Thayyil, A. R., T. Juturu, S. Nayak, and S. Kamath (2020). Pharmaceutical Co-crystallization: Regulatory Aspects, Design, Characterization, and Applications. *Advanced Pharmaceutical Bulletin*, **10**(2); 203

Thenmozhi, K. and Y. J. Yoo (2017). Enhanced Solubility of Piperine Using Hydrophilic Carrier-Based Potent Solid Dispersion Systems. *Drug Development and Industrial Pharmacy*, **43**(9); 1501–1509

Thong-Ngam, D., S. Choochuai, S. Patumraj, M. Chayanupatkul, and N. Klaikeaw (2012). Curcumin Prevents Indomethacin Induced Gastropathy in Rats. *World Journal of Gastroenterology: WJG*, **18**(13); 1479

Toyoda, T., L. Shi, S. Takasu, Y. M. Cho, Y. Kiriyama, A. Nishikawa, K. Ogawa, M. Tatematsu, and T. Tsukamoto (2016). Anti-inflammatory Effects of Capsaicin and Piperine on Helicobacter Pylori-Induced Chronic Gastritis in *Mongolian gerbils*. *Helicobacter*, **21**(2); 131–142

Wu, N., Y. Zhang, J. Ren, A. Zeng, and J. Liu (2020). Preparation of Quercetin Nicotinamide Cocrystals and Their Evaluation Under in Vivo and in Vitro Conditions. *RSC Advances*, **10**(37); 21852–21859

Wu, T., X. Zang, M. He, S. Pan, and X. Xu (2013). Structure Activity Relationship of Flavonoids on Their Anti-Escherichia Coli Activity and Inhibition of DNA Gyrase. *Journal of Agricultural and Food Chemistry*, **61**(34); 8185–8190

Yaffe, P. B., M. R. Power Coombs, C. D. Doucette, M. Walsh, and D. W. Hoskin (2015). Piperine, an Alkaloid from Black Pepper, Inhibits Growth of Human Colon Cancer Cells via G1 Arrest and Apoptosis Triggered by Endoplasmic Reticulum Stress. *Molecular Carcinogenesis*, **54**(10); 1070–1085

Yan, Y., J. M. Chen, and T. B. Lu (2013). Simultaneously Enhancing the Solubility and Permeability of Acyclovir by Crystal Engineering Approach. *CrystEngComm*, **15**(33); 6457–6460

Yang, D., J. Cao, L. Jiao, S. Yang, L. Zhang, Y. Lu, and G. Du (2020). Solubility and Stability Advantages of a New Cocrystal of Berberine Chloride with Fumaric Acid. *ACS Omega*, **5**(14); 8283–8292

Yang, Z. J., H. R. Wang, Y. L. Wang, Z. H. Zhai, L. W. Wang, L. Li, C. Zhang, and L. Tang (2019). Myricetin Attenuated Diabetes Associated Kidney Injuries and Dysfunction via Regulating Nuclear Factor (Erythroid Derived 2) Like 2 and Nuclear Factor-κB Signaling. *Frontiers in Pharmacology*, **10**;

647

Ying, H. Z., Y. H. Liu, B. Yu, Z. Y. Wang, J. N. Zang, and C. H. Yu (2013). Dietary Quercetin Ameliorates Nonalcoholic Steatohepatitis Induced by a High Fat Diet in Gerbils. *Food and Chemical Toxicology*, **52**; 53–60

Yu, M. S., J. Lee, J. M. Lee, Y. Kim, Y. W. Chin, J. G. Jee, Y. S. Keum, and Y. J. Jeong (2012). Identification of Myricetin and Scutellarein as Novel Chemical Inhibitors of The SARS Coronavirus Helicase, nsP13. *Bioorganic & Medicinal Chemistry Letters*, **22**(12); 4049–4054

Yusof, Y., C. Etti, and N. Chin (2015). Development of Nutraceutical Product. *International Journal on Advanced Science, Engineering and Information Technology*, **5**(3); 50–5

Zaini, E., L. Fitriani, F. Ismed, A. Horikawa, and H. Uekusa (2020a). Improved Solubility and Dissolution Rates in Novel Multicomponent Crystals of Piperine with Succinic Acid. *Scientia Pharmaceutica*, **88**(2); 21

Zaini, E., L. Fitriani, R. Y. Sari, H. Rosaini, A. Horikawa, and H. Uekusa (2019). Multicomponent Crystal of Mefenamic Acid and N-Methyl-D-Glucamine: Crystal Structures and Dissolution Study. *Journal of Pharmaceutical Sciences*, **108**(7); 2341–2348

Zaini, E., D. Riska, M. D. Oktavia, F. Ismed, and L. Fitriani (2020b). Improving Dissolution Rate of Piperine by Multicomponent Crystal Formation with Saccharin. *Research Journal of Pharmacy and Technology*, **13**(4); 1926–1930

Zarai, Z., E. Boujelbene, N. B. Salem, Y. Gargouri, and A. Sayari (2013). Antioxidant and Antimicrobial Activities of Various Solvent Extracts, Piperine and Piperic Acid from Piper Nigrum. *Lwt Food Science and Technology*, **50**(2); 634–641

Zhai, W. J., Z. B. Zhang, N. N. Xu, Y. F. Guo, C. Qiu, C. Y. Li, G. Z. Deng, and M. Y. Guo (2016). Piperine Plays an Anti-inflammatory Role in Staphylococcus Aureus Endometritis by Inhibiting Activation of NF-κB and MAPK Pathways in Mice. *Evidence-Based Complementary and Alternative Medicine*, **2016**; 1–10

Zhang, W., X. Li, T. Ye, F. Chen, X. Sun, J. Kong, X. Yang, W. Pan, and S. Li (2013). Design, Characterization, and in Vitro Cellular Inhibition and Uptake of Optimized Genistein-Loaded NLC for The Prevention of Posterior Capsular Opacification Using Response Surface Methodology. *International Journal of Pharmaceutics*, **454**(1); 354–366

Zhang, Y. N., H. M. Yin, Y. Zhang, D. J. Zhang, X. Su, and H. X. Kuang (2017a). Cocrystals of Kaempferol, Quercetin and Myricetin with 4, 4'-Bipyridine: Crystal Structures, Analyses of Intermolecular Interactions and Antibacterial Properties. *Journal of Molecular Structure*, **1130**; 199–207

Zhang, Y. N., H. M. Yin, Y. Zhang, D. J. Zhang, X. Su, and H. X. Kuang (2017b). Preparation of a 1: 1 Cocrystal of Genistein with 4, 4'-Bipyridine. *Journal of Crystal Growth*, **458**; 103–109

